

Harvesting Private Medical Images in Federated Learning Systems with Crafted Models

Shanghao Shi*, Md Shahedul Haque*, Abhijeet Parida[†], Marius George Linguraru^{†‡}, Y.Thomas Hou*,
Syed Muhammad Anwar^{†‡}, Wenjing Lou*

*Virginia Polytechnic Institute and State University, VA, USA

[†]Children’s National Hospital, DC, USA

[‡]George Washington University, DC, USA

Abstract—Federated learning (FL) allows a set of clients to collaboratively train a machine-learning model without exposing local training samples. In this context, it is considered to be privacy-preserving and hence has been adopted by medical centers to train machine-learning models over private data. However, in this paper, we propose a novel attack named MediLeak that enables a malicious parameter server to recover high-fidelity patient images from the model updates uploaded by the clients. MediLeak requires the server to generate an adversarial model by adding a crafted module in front of the original model architecture. It is published to the clients in the regular FL training process and each client conducts local training on it to generate corresponding model updates. Then, based on the FL protocol, the model updates are sent back to the server and our proposed analytical method recovers private data from the parameter updates of the crafted module. We provide a comprehensive analysis for MediLeak and show that it can successfully break the state-of-the-art cryptographic secure aggregation protocols, designed to protect the FL systems from privacy inference attacks. We implement MediLeak on the MedMNIST and COVIDx CXR-4 datasets. The results show that MediLeak can nearly perfectly recover private images with high recovery rates and quantitative scores. We further perform downstream tasks such as disease classification with the recovered data, where our results show no significant performance degradation compared to using the original training samples.

Index Terms—Federated Learning, Privacy Leakage, Medical Images.

I. INTRODUCTION

Federated learning (FL) has been regarded as a key enabling technology for the future implementation of AI-empowered medical diagnosis and treatment [1], [2], [3], [4], [5], [6], [7], [8]. FL allows medical centers to collaboratively train machine-learning models for various clinical tasks such as abnormality detection and disease classification, without sharing private patient information. This is very important because medical centers are bound to preserve patient privacy and their data usage is strictly restricted in many clinical applications. Under the FL framework, distributed training is set up in a way where hospitals that own private clinical data usually serve as clients, and a server – either hosted at one of the collaborating sites or maintained by a third party, integrates the model updates received from each client to orchestrate the federated learning paradigm. There are multiple open sources (such as NVFLARE [9] and OpenFL [10]) as well as commercial platforms (such as Rhino FCP [11]), designed to streamline the implementation

of FL. During the FL training process, only the model updates, which refer to either the gradients or parameter updates, are exchanged between the participant and the server, and all the private training samples are kept locally at the clinical site. Therefore, when first introduced, federated learning was considered to be privacy-preserving and the model updates are regarded as safe vectors that hide training samples’ private information [12], [13], [14], [15].

a) Existing Privacy Attacks: However, recent privacy attacks challenge this intuition as they demonstrate that a curious or malicious parameter server can extract useful information about the training samples such as their labels, membership information, and even training sample themselves from the model updates [16], [17], [18], [19], [20], [21], [22], [23], [24]. Of particular interest, the model inversion attacks (MIAs) [20], [22], [23], [24], [25] are a type of privacy attack aiming to recover the original training images. They take the individual model updates provided by the clients as inputs and reverse them back to the local training images. This could be detrimental in radiologic applications, where such an attack can reconstruct patient-specific data. Existing MIAs usually formulate this reverse process as an optimization problem and can achieve good recovery performance to recover high-fidelity training images from the model updates, when undergoing enough optimization iterations, which completely exposes the information that the FL system wants to protect. Fortunately, as the arms race between the attacker and defender goes on, a specialized multi-party computation (MPC) mechanism named secure aggregation (SA) protocol is proposed to prevent MIAs [26], [27], [28]. The fundamental idea of SA protocols is to use various cryptography primitives (e.g., secret sharing) to mask the individual model updates with random values but keep their summation identical to the pre-masked value so that the FL system can proceed to the training process without exposing individual model updates. As a result, the SA protocol prevents the MIAs from even obtaining the inputs (individual model updates) to the reverse processes, and the privacy of the FL systems is guaranteed. Moreover, existing MIAs are also facing scalability and efficiency challenges, as in practice they need the server to consume extensive resources (usually hundreds of seconds) to recover only a few images, making them hardly employable in real systems.

b) **Our Attack:** In this paper, we propose a novel attack name MediLeak that addresses the limitation of the existing works, making it a very practical attack and representing a privacy vulnerability of the FL systems. MediLeak can recover hundreds of training samples in a batch from the victim client simultaneously within a few seconds. MediLeak can also break the secure aggregation protocols as it can recover the training samples directly from the summation value of the model updates even though the individual ones are cryptographically masked. Technically, MediLeak is a two-phase attack including the attack preparation phase and the sample recovery phase. In the first phase, the attacker adds an additional two-linear layer module in front of the original model architecture and initializes the module with customized parameters before sending it to the clients. For the target victim, the attacker initializes the parameters of the two-layer module to form a “linear leakage” module with the help of an auxiliary dataset that has the same data format and distribution as the training samples. This “linear leakage” module is a powerful mathematical tool that can perfectly reverse its gradients back to its inputs, which are identical to the training samples because we place this module as the first component of the model architecture. For other clients, their two-layer modules’ parameters are crafted to form a “zero gradient” module, aiming to zero out their gradients and model updates. By doing so the aggregated model update is identical to the model update of the victim because all others are set to zero, rendering the SA protocols useless.

We implement MediLeak on the MedMNIST [29] and COVIDx CXR-4 [30] datasets and evaluate our attack performance using the recovery rate, structural similarity (SSIM) score, peak signal-to-noise ratio (PSNR) score, and attack time. The results show that MediLeak achieves excellent performance on both datasets to recover hundreds of images simultaneously with high recovery rates and quantitative scores, with only a few seconds of execution time. We visualize the recovered images and they are visually indistinguishable from the original images. We compare the performance of MediLeak with three existing MIAs. The results demonstrate that MediLeak achieves better quantitative scores and is much more efficient than them. We further feed the recovered images to downstream disease diagnosis tasks. Our results show that the recovered images achieve classification performance close to the original ones, demonstrating the effectiveness of our attack.

In summary, this paper makes the following contributions:

- 1) We propose MediLeak, a novel and powerful MIA that can recover large-batch and high-fidelity local training samples owned by the clients from the model updates efficiently when assuming the parameter server is a proactive attacker curious about the client’s private information, even when the system is protected by the state-of-the-art cryptography-based defense mechanisms.
- 2) Our attack represents a fundamental and practical privacy vulnerability of the current federated learning system as it leaks its participants’ private information, and promotes the urgent need for more effective defense mechanisms against such a powerful privacy attack.

- 3) We provide rigorous mathematical analysis and proof for our attack. Our attack is a closed-form attack and does not incur any computation-intensive optimization process, which reduces the computational costs significantly compared to existing model inversion attacks.
- 4) We implement MediLeak on medical image datasets under different practical assumptions in the FL systems. The results show that our attack can nearly perfectly recover the local training samples of the target victim with high performance in downstream clinical tasks.

II. BACKGROUND

A. Federated Learning

We consider for each training round t , there are n clients denoted by $\mathcal{C} = \{c_1, c_2, \dots, c_n\}$ to be selected by the parameter server S to collaboratively train a global model $G = f_\theta : \mathcal{X} \rightarrow \mathcal{Y}$, with each client c_i holds a local dataset D_i . In detail, the parameter server S first publishes the global model parameter θ^t to the clients. Then each client trains the received global model G_t for L_i^t local rounds over D_i to produce its model update δ_i^t . Note that when $L_i^t = 1$, the model update δ_i^t can be replaced by the gradient g_i^t . After that, the client c_i sends the model update δ_i^t back to the server S and the server employs the federated average (FedAVG) algorithm [12] to conduct the training process:

$$\theta^{t+1} = \sum_{i=1}^n \alpha_i \delta_i^t, \quad (1)$$

where α_i is the weight assigned to client c_i . The summation of all weights $\{\alpha_i\}_{i:c_i \in \mathcal{C}}$ is 1 and can be adjusted according to the size of local datasets D_i^t to avoid training bias. The server may also employ the FedSGD algorithm [12] as an alternative to conducting the training process. In the following sections, we will omit the notation t , because our attack and analysis are all conducted in a single FL training round.

B. Model Inversion Attacks

The model inversion attacks (MIAs) take the individual model updates δ_i as the inputs and aim to reconstruct them back to the local datasets D_i held by the clients. This reversion problem has been formalized as an optimization problem, represented as $\arg \min_{\hat{D}_i} [d(\nabla \hat{D}_i - \nabla D_i)]$, where \hat{D}_i refer to randomly initialized dummy samples and $d()$ refers to a distance function such as the second norm distance. To solve this optimization problem, [20] utilizes the L-BFGS optimizer to reconstruct the dummy samples iteratively step by step until reaching a good optimization point. It is further improved by an analytical method that aims to recover the ground-truth labels of dummy samples from the gradients [21], which significantly eases the optimization task and helps accomplish better attack performance. Later works improve the optimization tools and focus on recovering larger batches of images on more practical machine learning models such as the ResNet [22], [23], [31], [32]. However, their recovery sizes are still restricted to the scale of tens, representing a scalability challenge. Moreover, all the aforementioned MIAs require costly iterative optimization

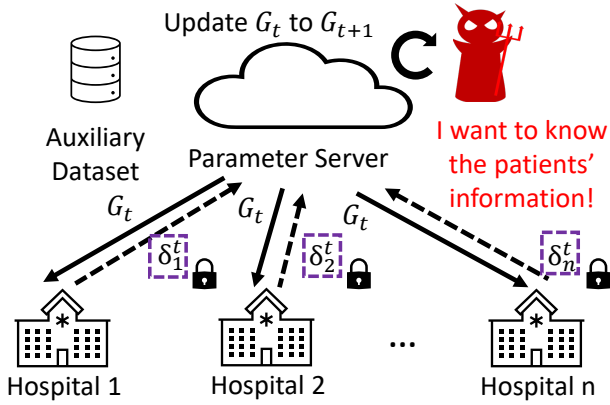


Fig. 1. Threat Model. The server is considered to be a malicious attacker. The secure aggregation protocol is considered to be in place to protect the individual model updates.

methods in their design, which unfortunately, introduce a very large overhead to recover each batch of input images. These methods also cannot bypass the current SA protocols.

C. Secure Aggregation

To enhance the privacy of the federated learning systems, Bonawitz et al. [26] propose a new type of specialized MPC mechanism named the secure aggregation (SA) protocols to fulfill an abstract function of masking individual model updates δ_i with random bits while keeping the summation of the masked values $\sum_{i=1}^n u_i$ identical to the pre-masked one $\sum_{i=1}^n \delta_i$. Therefore, despite variations of detailed cryptographic design, all SA protocols ensure that the server *cannot* obtain the individual model updates δ_i to launch any model inversion attacks, but can proceed with the FL training process with the aggregated model update $\sum_{i=1}^n u_i$, which is identical to $\sum_{i=1}^n \delta_i$. Since its initial introduction, the SA protocols have been continuously refined to incorporate other properties including communication efficiency, drop-out resilience [33], [34], [35], [36], and security against malicious clients [27], [28], making it the current state-of-the-art privacy protection mechanism for FL systems.

Secure Aggregation under Challenge: Under the honest-but-curious attack model, the SA protocols have proven to be secure against various MIAs. However, recent works adopt a stronger attack model to assume a *proactive* attacker that modifies the global model’s parameters and even its architecture before publishing it to the clients. Under this assumption, [25] proposes a novel attack that retrieves a target individual model update from the aggregated result that breaks the SA protocols. The fundamental idea of this novel attack is to craft the model parameters to adversarial models and distribute different adversarial models to different clients strategically. The adversarial models are crafted to ensure that only the model update of the victim client is preserved while all the others are zeroed out. The limitation of this attack is that it incorporates a costly optimization process in its design, which introduces too much attack overheads. [24] proposes another

attack method to add crafted modules before the original model architecture. These additional modules are crafted with delicate mathematical designs to ensure that the model gradients can be perfectly reversed back to inputs whenever the server receives any model updates. The limitation of this attack is that the attacker cannot link the recovered images to their owners, which means the SA protocols still preserve a certain level of privacy, known as “privacy by shuffling”.

In summary, the security of the SA protocols is challenged by the advanced attacks under the proactive attacker assumption. In our design, we adopt this fundamental attack assumption to break the SA protocol and address various limitations of the existing work at the same time.

III. THREAT MODEL

In Fig.1 we demonstrate the threat model of our attack. We consider the parameter server S to be a malicious party that is curious about the training samples held by clients (e.g., private patient information). We consider the parameter server to be a proactive attacker and can actively modify model parameters and architectures from G to \hat{G} to achieve the attack goals, following the same assumption as [25], [24], [37]. We assume the communication channels between the server and clients are secured and all messages can be authenticated. We assume the state-of-the-art SA protocols are in place and the server can only get access to the aggregated model updates $\sum_{i=1}^n \delta_i$ without knowing anything about the individual values δ_i . We consider the attacker is able to collect or obtain an auxiliary dataset D_{aux} that has the same data format and can represent the target dataset well. The attacker can leverage various online resources such as publicly available datasets, image searching tools, and image generative tools to fulfill this requirement. For our use case, the availability of public chest X-ray datasets makes this task trivial. The goal of the attacker is to recover the local data samples of a target client c_{target} from the aggregated model updates $\sum_{i=1}^n \delta_i$. This can be mathematically expressed as: $D_{target} = Reverse(\sum_{i=1}^n \delta_i, \hat{G})$.

IV. ATTACK METHOD

A. Attack Overview

We decompose the complex recovery problem into two different tasks including the *individual model update retrieval* and *efficient model update reversion*. To accomplish them, we require the attacker to place an additional two-linear-layer module L_{adv} with the rectified linear unit (ReLU) activation function in between at the beginning of the original global model, i.e. $\hat{G} = G \oplus L_{adv}$. The dimension of this module is identical to the image dimension. We require the attacker to initialize the parameters of the linear module L_{adv} to form different adversarial modules and distribute them to different clients accordingly. For all the other clients except the victim, the attacker crafts the “zero gradient” modules L_{zero} to ensure that the gradients and model updates of these clients are always zero, i.e. $\hat{G}_{others} = G \oplus L_{zero}$. By doing this, the attacker guarantees that only the model update of the victim client is exposed, accomplishing task one. For the victim client,

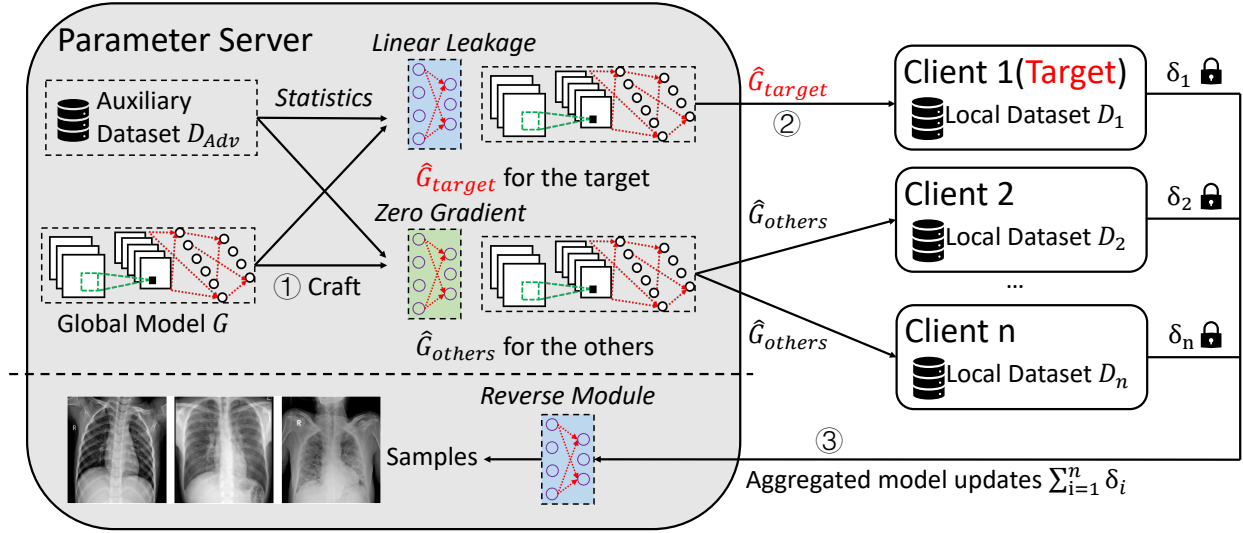


Fig. 2. MediLeak attack flow. MediLeak is a two-phase attack. In the first preparation phase, the attacker generates the adversarial global model. In the second reconstruction phase, the attacker sends the adversarial models to the clients and recovers the local samples when it receives their feedback.

the attacker crafts a “linear leakage” module L_{linear} , aiming to reverse its model update back to local training samples efficiently, i.e. $\hat{G}_{target} = G \oplus L_{linear}$. This module requires an auxiliary dataset to help generate essential parameters and can ensure that samples are *perfectly recovered* with a mathematical proof, accomplishing task two. Detailed attack flow and module designs are introduced in the next section.

B. Detailed Attack Flow

We demonstrate the attack flow in Fig.2. MediLeak is a two-phase attack including 1) attack preparation and 2) sample reconstruction phases. In the attack preparation phase, the attacker crafts the adversarial global model \hat{G} and initializes it with different model parameters including L_{zero} and L_{linear} (step ①) before publishing them to different clients (step ②). Then in the second phase, the attacker collects the aggregated model updates and uses an analytical method to reverse it back to local training samples (step ③).

a) Attack Preparation: In this phase, the attacker crafts both the “linear leakage” module and “zero gradient” module once at the outset. Both modules require the estimation of essential parameters of a representative auxiliary dataset D_{aux} . In detail, the attacker first estimates the cumulative density function (CDF) of the brightness feature $h(x)$ of the auxiliary dataset D_{aux} , denoted by $\psi(h(x))$, to represent the CDF of the local training dataset (which is unavailable), where x refers to the input vector. After that, the attacker divides the distribution ψ into equally k bins by calculating $h_j = \psi^{-1}(j/k)$ where $j \in \{1, 2, \dots, k\}$, ψ^{-1} refers to the inverse function of ψ , and k equals to the neuron number of the first linear layer. By doing so, the brightness of a random input vector x denoted by $h(x)$ will have the same probability of falling into each bin. This bin vector $\mathbf{H} = [h_1, h_2, \dots, h_k]$ is the key vector to craft the model parameters of the adversarial global model \hat{G} to form both attack modules.

Linear Leakage Module: Assuming the weight and bias matrix of the two-layer module L_{adv} are w_1, b_1 and w_2, b_2 respectively. For the target victim, the attacker initializes the “linear leakage” module L_{linear} with the following steps: (1) having w_1 ’s row vectors all identical to $[\frac{1}{d}, \frac{1}{d}, \dots, \frac{1}{d}]$, where d refers to the dimension of the input images, resulting in calculating the brightness feature on each neuron when the local training images are sent into the model during the FL training process; (2) having the bias b_1 identical the opposite value of \mathbf{H} , i.e., $b_1 = -\mathbf{H}$; (3) having all row vectors of w_2 the same.

Zero Gradient Module: The “zero gradient” module is initialized in the same way as the “linear leakage” module except in step (2), in which the attacker has the bias vector b_1 equal to $\mathbf{H}' = -[h_k, h_k, \dots, h_k]$. By doing so, the output of the first linear layer will always be smaller than zero because h_k is the largest possible brightness and all possible input x ’s brightness is smaller than it. Considering we use the ReLU activation function after the first layer, the input to the second layer and the gradients of the first layer shall always be zero because of the ReLU function’s mathematical property. This results in zero model updates for all clients except the target victim. Therefore, the aggregated model updates are identical to the model updates of the victim client, i.e. $\sum_{i=1}^n \delta_i = \mathbf{0} + \mathbf{0} + \dots + \mathbf{0} + \delta_{target} = \delta_{target}$, exposing the model updates of the target victim.

b) Sample Reconstruction: The sample reconstruction phase can be treated as the actual *attack phase*, in which the parameter server disseminates the crafted global models \hat{G} to all clients and recovers the local samples of the target victim D_{target} according to the aggregated model updates $\sum_{i=1}^n \delta_i$ provided by all clients.

More specifically, with the help of the “zero gradient” module, the aggregated model update $\sum_{i=1}^n \delta_i$ the attacker obtains is identical to the model update of the victim client

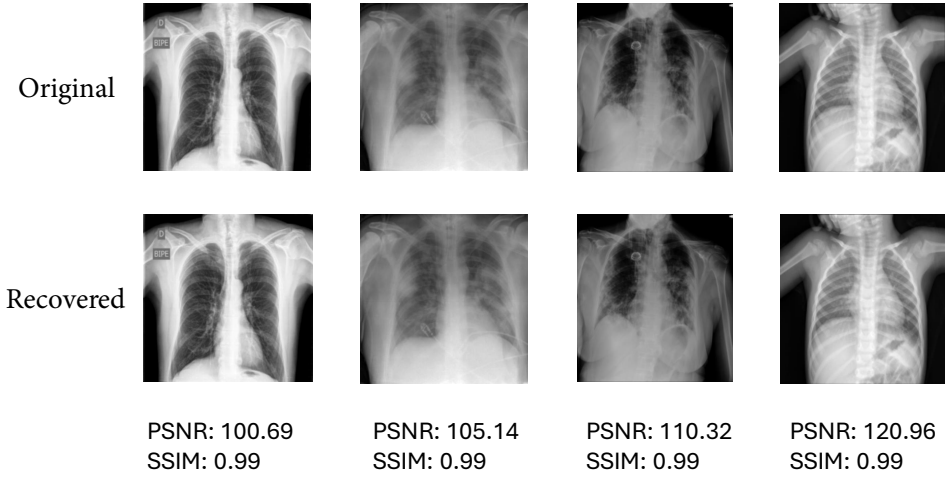


Fig. 3. Recovered examples from the COVIDx CXR-4 dataset. The original images are shown in the first row and the recovered ones are shown in the second. High PSNR and SSIM scores denote nearly perfect recovery of the original images.

δ_{target} , even though the SA protocols are in place. We further argue that the attacker can accurately estimate the gradients from the model update δ_{target} as it equals local iterations of the gradients [12], [38]. We define the gradients of the first two layers of the target victim as g_{w_1}, g_{b_1} and g_{w_2}, g_{b_2} respectively. The attacker can calculate the following equation to reconstruct the input samples, for $l \in \{1, 2, \dots, k\}$:

$$(g_{w_1}^{(l+1)} - g_{w_1}^{(l)}) / (g_{b_1}^{(l+1)} - g_{b_1}^{(l)}), \quad (2)$$

where specially we have $g_{w_1}^{(k+1)}$ and $g_{b_1}^{(k+1)}$ equal zero.

Analysis: Equ. 2 creates k recovery bins to recover input images. Fortunately, when $k \geq m$, where m refers to the size of the target dataset, each local training sample in the dataset will be *perfectly recovered* within a certain bin ranging from 1 to k . Here perfect recovery means that the inputs are analytically calculated through closed-form mathematical equations. A rigorous mathematical proof for this property is provided in the next section. However, when $k < m$, there will be recovery conflicts, and some recovered samples are mixed with each other in certain bins, resulting in degraded recovery rates and quality. We argue this does not mean the total failure of the image reconstruction task. We will later demonstrate that in this scenario the attack performance gradually decreases and the attack remains to achieve decent performance when attack parameter k is about the same scale as m .

We regard the attack parameter k as the key factor that affects reconstruction performance. Fortunately, from the attacker’s perspective, this parameter is controlled and adjustable. The attacker can have a larger k (i.e. craft larger linear layers) for large datasets and a smaller one for small datasets according to different attack scenarios to ensure that there are enough recovery bins for all samples. Regarding attack complexity, both the attack preparation and sample reconstruction phases only involve closed-form mathematical calculations that are super efficient to be conducted.

C. Proof of Correctness:

Considering the input x_p falls in the p^{th} largest bin, i.e. the brightness of x_p denoted by $h(x_p)$ satisfies $h_p < h(x_p) < h_{p+1}$. Then the following equation holds:

$$\begin{aligned} \frac{g_{w_1}^{(p+1)} - g_{w_1}^{(p)}}{g_{b_1}^{(p+1)} - g_{b_1}^{(p)}} &= \frac{\nabla_{w_1(p+1)} L - \nabla_{w_1(p)} L}{\nabla_{b_1(p+1)} L - \nabla_{b_1(p)} L} \\ &= \frac{\frac{\partial L}{\partial y_{p+1}} \frac{\partial y_{(p+1)}}{\partial w_1(p+1)} - \frac{\partial L}{\partial y_p} \frac{\partial y_{(p)}}{\partial w_1(p)}}{\frac{\partial L}{\partial y_{p+1}} \frac{\partial y_{(p+1)}}{\partial b_1(p+1)} - \frac{\partial L}{\partial y_p} \frac{\partial y_{(p)}}{\partial b_1(p)}} \\ &= \frac{\sum_{v=1}^p \frac{\partial L}{\partial y_{p+1}} x_v - \sum_{v=1}^{p-1} \frac{\partial L}{\partial y_p} x_v}{\sum_{v=1}^p \frac{\partial L}{\partial y_{p+1}} - \sum_{v=1}^{p-1} \frac{\partial L}{\partial y_p}} \\ &= \frac{\frac{\partial L}{\partial y_p} x_p}{\frac{\partial L}{\partial y_p}} = x_p \end{aligned} \quad (3)$$

where L is the loss function, y is the output of the first linear layer, and $\frac{\partial L}{\partial y_{p+1}} = \frac{\partial L}{\partial y_p}$ because we let the row vectors of the w_2 matrix identical. This equation implies x_p is perfectly recovered from the gradients of the first linear layer. Because \mathbf{H} covers the whole distribution range of the brightness feature, each input image will fall into one bin and thus can be recovered in this way as long as the image number is smaller than k .

V. EVALUATION

A. Experimental Settings:

We implemented MediLeak on the PyTorch platform. We ran all the experiments on a server equipped with an Intel Core i7-12700K CPU 3.60GHzX12, one NVIDIA GeForce RTX 3080 Ti GPU, and Ubuntu 20.04.6 LTS.

We use three evaluation metrics including the recovery rate, the peak signal-to-noise ratio (PSNR) score, and the structural similarity index measure (SSIM) score, following the

TABLE I
THE RECONSTRUCTION PERFORMANCE OF MEDILEAK OVER DIFFERENT DATASETS AND RECONSTRUCTION BATCH SIZES. THE RATE (SAMPLE RECOVERY RATE) IS ON A SCALE OF 1.00

Batch Size	Dataset	Pixel Size	Rate	PSNR	SSIM	Time (in sec)
100	ChestMNIST(pneumonia)	28x28	1.0	112.574	0.99	0.742
	COVIDx CXR-4	224x224	0.95	120.795	0.99	6.022
200	ChestMNIST(pneumonia)	28x28	0.96	102.722	0.99	0.936
	COVIDx CXR-4	224x224	0.89	114.98	0.99	7.003
300	ChestMNIST(pneumonia)	28x28	0.957	97.405	0.99	0.95
	COVIDx CXR-4	224x224	0.88	105.12	0.99	8.121
400	ChestMNIST(pneumonia)	28x28	0.955	93.713	0.99	1.020
	COVIDx CXR-4	224x224	0.86	97.30	0.99	8.762
500	ChestMNIST(pneumonia)	28x28	0.964	87.019	0.99	1.016
	COVIDx CXR-4	224x224	0.81	95.86	0.99	9.763

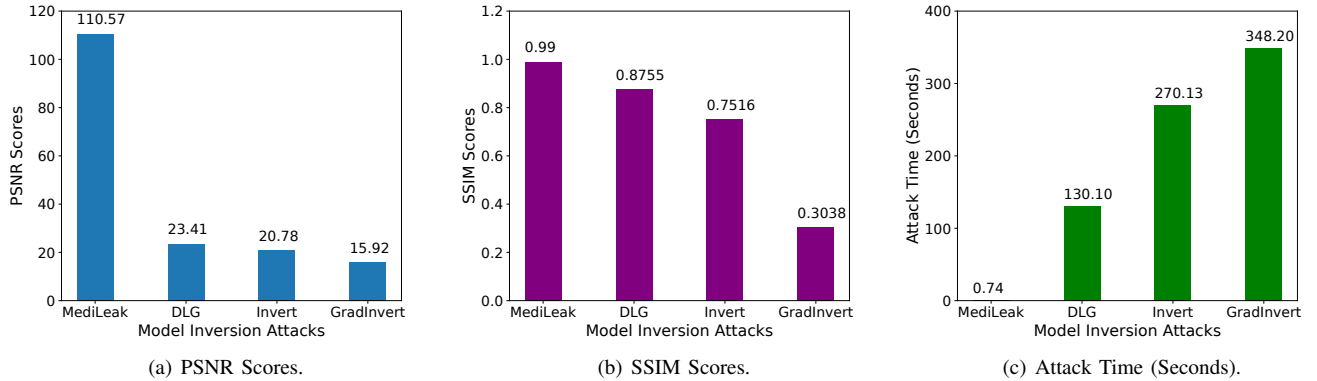


Fig. 4. The attack performance comparison between MediLeak with other model inversion attacks.

convention of the existing works [20], [21], [22], [23], [24] to evaluate our attack. More specifically, the successful recovery of samples is measured by observing the PSNR and SSIM scores between the original input samples and the reconstructed ones, and checking whether those scores exceed a certain threshold th . In our work, we choose $th = 20$ for PSNR and $th = 0.9$ for SSIM because these thresholds are enough to ensure that the recovered images are visually clear for the attacker to extract all meaningful content from them.

We consider the FL system to have 5 clients with one of them being the attack target per training round and each client conducts 5 local iterations before generating individual model updates. We randomly select 10% of the training set as the auxiliary dataset and aim to recover samples in the test set, which have *no intersection* with the auxiliary dataset. We assume the test set is partitioned and owned by the 5 clients locally to serve as the local datasets.

We choose the ChestMNIST dataset from the MedMNIST package [29] and the COVIDx CXR-4 dataset [30] as our experiment datasets. The ChestMNIST dataset comprises frontal view X-ray images ($1 \times 28 \times 28$) of 30805 unique patients with 14 disease labels and we selected data samples related to pneumonia to conduct our experiments, including 78468 training samples and 22433 testing samples. The COVIDx CXR-4 dataset also consists of frontal view chest X-ray images with higher dimensions (resized to $1 \times 224 \times 224$) and labels about

whether the patient is COVID-positive. The training set contains 67863 samples and the testing set contains 8482 samples.

B. Reconstruction Results

In Tab. I we demonstrate the performance of MediLeak over different recovery batch sizes (i.e. the number of samples recovered simultaneously held by the target victim) ranging from 100 to 500 images. We can observe that both the recovery rate (i.e. the ratio of successfully recovered images) and the quantitative scores (i.e. the PSNR and SSIM scores) decrease when the recovered batch size increases. This is expected because the larger the recovery batch size, the more difficult the recovery task to conduct. But in general, MediLeak achieves high recovery rates (> 0.8) and quantitative scores (PSNR > 80 and SSIM > 0.9) for both datasets under all recovery batch sizes. Particularly, the SSIM scores (ranging from 0 to 1) remain to be 0.99 for all settings, because of the recovery excellency. This can be further verified by the recovered samples we visualized in Fig. 3, in which we plot the original images in the first row and the recovered ones in the second. We find that the recovered images are of high quality and cannot be visually distinguished from the original ones, even for some detailed small marks and notations. In Tab. I we also demonstrate the attack time (in seconds). We find that the attack time is monotonically increasing with respect to the recovery batch size. For the largest batch size (i.e. 500 images) over the complex COVIDx

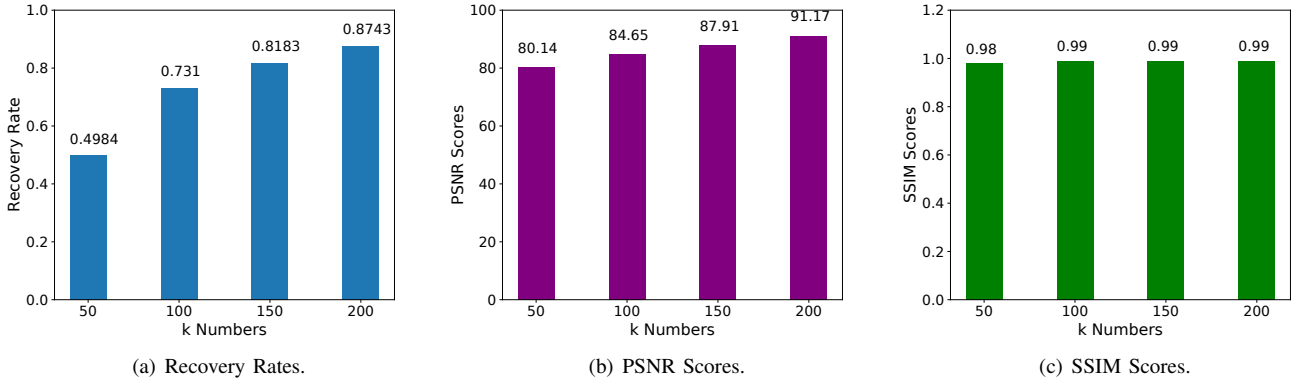


Fig. 5. The performance of MediLeak over different k numbers. k refers to the neuron number of the first linear layer.

TABLE II

DOWNSTREAM BINARY CLASSIFICATION TASK ON THE COVID DATASET WITH A PRE-TRAINED (WITH CXR-3 DATASET) ViT MODEL. TPR: TRUE POSITIVE RATE, TNR: TRUE NEGATIVE RATE, ACC: ACCURACY, AUC: AREA UNDER RECEIVER OPERATING CHARACTERISTIC CURVE, AUPR: AREA UNDER PRECISION RECALL CURVE.

Model	Image	AUPR	TNR	TPR	ACC	AUROC
ViT-S (SSL)	Original	0.937	0.800	0.857	0.829	0.905
	Recovered	0.921	0.900	0.710	0.805	0.919
ViT-S (Fine-tuned)	Original	0.974	0.970	0.930	0.950	0.969
	Recovered	0.965	0.886	0.938	0.912	0.966

CXR-4 dataset, it only takes the attacker less than 10 seconds to fulfill the recovery task, indicating that MediLeak is very effective.

C. Benchmark Comparison

We compare MediLeak’s attack performance with three optimization-based model inversion attacks (MIAs) including the DLG/iDLG [20], [21], InvertGradient [22], and GradInversion [23] attacks (denoted as DLG, Invert, and GradInvert respectively) over the MedMNIST dataset for one small batch of input images. We compare the PSNR scores, SSIM scores, and the attack time between the three attacks and our work. The results are demonstrated in Fig. 4. We can find that our attack achieves much better PSNR scores and SSIM scores than the existing MIAs, indicating that our attack can reconstruct samples with better quality. At the same time, our attack consumes significantly less time than the current MIAs. Particularly, the existing attacks consume a few hundred seconds to reconstruct one batch of samples, while our attack only requires less than one second, which reduces the current cost by two orders of magnitude. The reason why our attack is much more efficient is that our attack only involves closed-form mathematical calculations while the other three attacks require costly iterative-based optimization methods. However, there is no free lunch and we clarify that the three benchmark works adopt an honest-but-curious attack model, which does not allow the attacker to modify the model parameters and architecture as we did.

D. Performance Affecting Factors

As we have discussed at the end of section IV. The neuron number k of the first linear layer is the key factor that affects the performance of MediLeak. In this section, we fix the reconstruction batch size to 100 to evaluate the attack performance under different k settings. We demonstrate the recovery rates and the quantitative scores (i.e. the PSNR score and SSIM score) of the **successfully recovered** samples. For the recovery rate, we observe that it is monotonically increasing with k and obtains relatively high recovery rates when $k \geq m$ ($m=100$ in this experiment). This is consistent with our theoretical analysis as more bins (larger k) will decrease the recovery conflict probability and increase the recovery success rates. For the PSNR and SSIM scores, we observe that the successful samples continuously maintain excellent reconstruction quality (i.e. obtaining very high scores) under different settings, while the unsuccessful ones achieve poor scores lower than the threshold (i.e. $PSNR < 20$ and $SSIM < 0.9$). This indicates that our attack demonstrates a binary recovery property, meaning that the recovery task either fails to obtain nothing or succeeds in recovering images with perfect quality.

E. Downstream Tasks

To further evaluate the performance of our attack on clinically relevant downstream tasks, we perform a binary disease classification (the detection of COVID-19) task on both the recovered samples and the actual samples. We use the state-of-the-art vision transformer model (ViT-S) (embedding size=368, number of heads=6, 22M parameters) pre-trained by self-

supervised learning (SSL) technique on 30k COVIDx CXR-3 samples and fine-tuned on the RSNA-RICORD part of the dataset to perform the classification task [39] and evaluate it on the COVIDx CXR-4 dataset. We demonstrate the performance in Tab.II. We use widely used machine learning metrics to evaluate the classification performance and we find that the recovered images achieve nearly the same performance as the original ones. This shows that our reconstruction process is highly successful in keeping all semantic meaning within the images and the reconstructed images can be used to perform any potential clinical analysis, which further indicates the severity of the privacy threat imposed by our attack. We consider it a very practical attack scenario for a curious party, which either can be the medical federated learning’s participants or a third-party service provider (who provides the necessary platform, computation resource, and other FL infrastructures) to launch our attack to first reconstruct the sensitive medical images and then feed them to certain downstream analysis tasks to obtain further information about of the victims.

VI. DISCUSSION AND FUTURE WORK

Auxiliary Dataset: The number and quality of samples in the auxiliary data D_{aux} affect the performance of our attack. The dataset is used in the attack preparation phase for estimating essential attack parameters before crafting the “zero gradient” and “linear leakage” modules. In the ideal case, the auxiliary dataset shall have the same data distribution as the target victim’s local dataset or the auxiliary dataset is more representative. It may be a challenge for the general vision tasks to find such a representative auxiliary dataset. However, for the medical images, this does not pose a barrier because the medical images such as the CT scanning images of humans are fixed to have the same data format and similar common features. The attacker can easily obtain representative datasets released for research purposes on the Internet. Moreover, because the attacker is a participant in the FL system, we consider he may even collude with others to obtain this auxiliary dataset.

Attack Scalability: Our attack is a single-round attack and we have already demonstrated that it can efficiently reconstruct hundreds of samples simultaneously. However, we argue that the attacker can boost his attack scalability performance to launch MediLeak in multiple or continuous FL training rounds. In this way, the attacker can “harvest” the local training samples of a single or even multiple clients continuously to obtain more sensitive data samples. The recovery rate of certain images in the local datasets will also increase, as they may eventually be reconstructed during the continuous multi-round attacks even though they escape the recovery process of a single round.

Defense Mechanisms: One intuitive but effective defense against our attack is to let the clients proactively check the consistency of the model parameters and architectures during the FL training process, rather than blindly believe in the privacy guarantee of the FL systems and give full trust in the FL service providers, which unfortunately, in the current fact for the medical FL systems. However, we argue that our attack can be launched in the initial training rounds or even

just the first training round to preserve attack stealthiness. This is because in the initial training rounds, everything is randomly initialized and it is difficult for the defender to distinguish the malicious behaviors from randomly initialized benign patterns.

Other Medical Records: In this work, we focus on the reconstruction problem of the *medical images* within the secure FL systems under the protection of advanced cryptography mechanisms, demonstrating a serious privacy threat to the current systems. But we notice that the other formats of medical records such as tabular and human language data also contain a huge amount of sensitive and private information. In practice, these records usually involve more detailed personal information such as the patient’s name, address, phone number, and health conditions. We consider the privacy issue of these data records, particularly whether these records can be reconstructed and exposed to a malicious party when they are used in a federated learning system as a very important security and privacy problem. We consider our method to provide a fundamental idea and attack flow about how to recover sensitive client-owned records from the aggregated model updates. However, we acknowledge that such a complex reconstruction problem involving multi-modality data records is non-trivial and deserves a lot of efforts. We leave this as the future direction of our work.

VII. CONCLUSION

In this paper, we present MediLeak—a powerful MIA that breaks the privacy-preserving feature of the current secure federated learning systems protected by the state-of-the-art SA protocols by accurately and efficiently recovering local training samples owned by the clients, resulting in a complete exposure of the patient’s private information. Our attack requires the attacker to first modify the global model architecture and initialize it to form different adversarial modules before publishing it to the clients. Then according to normal FL procedure, the clients train the received global model with their local datasets to provide model updates for the server. Upon recipient, we devise an efficient analytical method to reverse the collected aggregated model updates back to the local training samples without relying upon any costly optimization methods. We implement our attack on two practical medical image datasets and evaluate the attack performance under different settings. The experiment results demonstrate that our attack achieves excellent reconstruction performance, and outperforms the existing optimization-based MIAs. Our attack represents a practical vulnerability of the current medical FL systems, making the community rethink the privacy guarantee of the current systems, and calling for effective defense against such kinds of advanced MIAs.

REFERENCES

- [1] T. S. Brisimi, R. Chen, T. Mela, A. Olshevsky, I. C. Paschalidis, and W. Shi, “Federated learning of predictive models from federated electronic health records,” *International journal of medical informatics*, vol. 112, pp. 59–67, 2018.

- [2] N. Rieke, J. Hancox, W. Li, F. Milletari, H. R. Roth, S. Albarqouni, S. Bakas, M. N. Galtier, B. A. Landman, K. Maier-Hein, *et al.*, “The future of digital health with federated learning,” *NPJ digital medicine*, vol. 3, no. 1, p. 119, 2020.
- [3] M. J. Sheller, B. Edwards, G. A. Reina, J. Martin, S. Pati, A. Kotrotsou, M. Milchenko, W. Xu, D. Marcus, R. R. Colen, *et al.*, “Federated learning in medicine: facilitating multi-institutional collaborations without sharing patient data,” *Scientific reports*, vol. 10, no. 1, p. 12598, 2020.
- [4] M. Adnan, S. Kalra, J. C. Cresswell, G. W. Taylor, and H. R. Tizhoosh, “Federated learning and differential privacy for medical image analysis,” *Scientific reports*, vol. 12, no. 1, p. 1953, 2022.
- [5] S. Pati, U. Baid, M. Zenk, B. Edwards, M. Sheller, G. A. Reina, P. Foley, A. Gruzdev, J. Martin, S. Albarqouni, *et al.*, “The federated tumor segmentation (fets) challenge,” *arXiv preprint arXiv:2105.05874*, 2021.
- [6] I. Dayan, H. R. Roth, A. Zhong, A. Harouni, A. Gentili, A. Z. Abidin, A. Liu, A. B. Costa, B. J. Wood, C.-S. Tsai, *et al.*, “Federated learning for predicting clinical outcomes in patients with covid-19,” *Nature medicine*, vol. 27, no. 10, pp. 1735–1743, 2021.
- [7] D. C. Nguyen, Q.-V. Pham, P. N. Pathirana, M. Ding, A. Seneviratne, Z. Lin, O. Dobre, and W.-J. Hwang, “Federated learning for smart healthcare: A survey,” *ACM Computing Surveys (Csur)*, vol. 55, no. 3, pp. 1–37, 2022.
- [8] D. Ng, X. Lan, M. M.-S. Yao, W. P. Chan, and M. Feng, “Federated learning: a collaborative effort to achieve better medical imaging models for individual sites that have small labelled datasets,” *Quantitative Imaging in Medicine and Surgery*, vol. 11, no. 2, p. 852, 2021.
- [9] H. R. Roth, Y. Cheng, Y. Wen, I. Yang, Z. Xu, Y.-T. Hsieh, K. Kersten, A. Harouni, C. Zhao, K. Lu, *et al.*, “Nvidia flare: Federated learning from simulation to real-world,” *arXiv preprint arXiv:2210.13291*, 2022.
- [10] G. A. Reina, A. Gruzdev, P. Foley, O. Perepelkina, M. Sharma, I. Davidyuk, I. Trushkin, M. Radionov, A. Mokrov, D. Agapov, *et al.*, “Openfl: An open-source framework for federated learning,” *arXiv preprint arXiv:2105.06413*, 2021.
- [11] K. Stephens, “Rhino health raises 5 million to improve ai workflows in healthcare using federated learning,” *AXIS Imaging News*, 2021.
- [12] B. McMahan, E. Moore, D. Ramage, S. Hampson, and B. A. y Arcas, “Communication-efficient learning of deep networks from decentralized data,” in *Artificial intelligence and statistics*, pp. 1273–1282, PMLR, 2017.
- [13] C. Zhang, Y. Xie, H. Bai, B. Yu, W. Li, and Y. Gao, “A survey on federated learning,” *Knowledge-Based Systems*, vol. 216, p. 106775, 2021.
- [14] K. Wei, J. Li, M. Ding, C. Ma, H. Su, B. Zhang, and H. V. Poor, “User-level privacy-preserving federated learning: Analysis and performance optimization,” *IEEE Transactions on Mobile Computing*, vol. 21, no. 9, pp. 3388–3401, 2021.
- [15] B. Pfitzner, N. Steckhan, and B. Arnrich, “Federated learning in a medical context: a systematic literature review,” *ACM Transactions on Internet Technology (TOIT)*, vol. 21, no. 2, pp. 1–31, 2021.
- [16] M. Nasr, R. Shokri, and A. Houmansadr, “Comprehensive privacy analysis of deep learning: Passive and active white-box inference attacks against centralized and federated learning,” in *2019 IEEE symposium on security and privacy (SP)*, pp. 739–753, IEEE, 2019.
- [17] C. Fu, X. Zhang, S. Ji, J. Chen, J. Wu, S. Guo, J. Zhou, A. X. Liu, and T. Wang, “Label inference attacks against vertical federated learning,” in *31st USENIX security symposium (USENIX Security 22)*, pp. 1397–1414, 2022.
- [18] X. Luo, Y. Wu, X. Xiao, and B. C. Ooi, “Feature inference attack on model predictions in vertical federated learning,” in *2021 IEEE 37th International Conference on Data Engineering (ICDE)*, pp. 181–192, IEEE, 2021.
- [19] L. Wang, S. Xu, X. Wang, and Q. Zhu, “Eavesdrop the composition proportion of training labels in federated learning,” *arXiv preprint arXiv:1910.06044*, 2019.
- [20] L. Zhu, Z. Liu, and S. Han, “Deep leakage from gradients,” *Advances in neural information processing systems*, vol. 32, 2019.
- [21] B. Zhao, K. R. Mopuri, and H. Bilen, “idlg: Improved deep leakage from gradients,” *arXiv preprint arXiv:2001.02610*, 2020.
- [22] J. Geiping, H. Bauermeister, H. Dröge, and M. Moeller, “Inverting gradients-how easy is it to break privacy in federated learning?,” *Advances in Neural Information Processing Systems*, vol. 33, pp. 16937–16947, 2020.
- [23] H. Yin, A. Mallya, A. Vahdat, J. M. Alvarez, J. Kautz, and P. Molchanov, “See through gradients: Image batch recovery via gradinversion,” in *Proceedings of the IEEE/CVF Conference on Computer Vision and Pattern Recognition*, pp. 16337–16346, 2021.
- [24] L. Fowl, J. Geiping, W. Czaja, M. Goldblum, and T. Goldstein, “Robbing the fed: Directly obtaining private data in federated learning with modified models,” *arXiv preprint arXiv:2110.13057*, 2021.
- [25] D. Pasquini, D. Francati, and G. Ateniese, “Eluding secure aggregation in federated learning via model inconsistency,” in *Proceedings of the 2022 ACM SIGSAC Conference on Computer and Communications Security*, pp. 2429–2443, 2022.
- [26] K. Bonawitz, V. Ivanov, B. Kreuter, A. Marcedone, H. B. McMahan, S. Patel, D. Ramage, A. Segal, and K. Seth, “Practical secure aggregation for privacy-preserving machine learning,” in *proceedings of the 2017 ACM SIGSAC Conference on Computer and Communications Security*, pp. 1175–1191, 2017.
- [27] K. Pillutla, S. M. Kakade, and Z. Harchaoui, “Robust aggregation for federated learning,” *IEEE Transactions on Signal Processing*, vol. 70, pp. 1142–1154, 2022.
- [28] L. Burkharter, H. Lycklama, A. Viand, N. Küchler, and A. Hithnawi, “Rofl: Attestable robustness for secure federated learning,” *arXiv e-prints*, pp. arXiv:2107, 2021.
- [29] J. Yang, R. Shi, D. Wei, Z. Liu, L. Zhao, B. Ke, H. Pfister, and B. Ni, “Medmnist v2-a large-scale lightweight benchmark for 2d and 3d biomedical image classification,” *Scientific Data*, vol. 10, no. 1, p. 41, 2023.
- [30] L. Wang, Z. Q. Lin, and A. Wong, “Covid-net: A tailored deep convolutional neural network design for detection of covid-19 cases from chest x-ray images,” *Scientific reports*, vol. 10, no. 1, p. 19549, 2020.
- [31] J. Lu, X. S. Zhang, T. Zhao, X. He, and J. Cheng, “April: Finding the achilles’ heel on privacy for vision transformers,” in *Proceedings of the IEEE/CVF Conference on Computer Vision and Pattern Recognition*, pp. 10051–10060, 2022.
- [32] Y. Wen, J. Geiping, L. Fowl, M. Goldblum, and T. Goldstein, “Fishing for user data in large-batch federated learning via gradient magnification,” *arXiv preprint arXiv:2202.00580*, 2022.
- [33] J. H. Bell, K. A. Bonawitz, A. Gascón, T. Lepoint, and M. Raykova, “Secure single-server aggregation with (poly) logarithmic overhead,” in *Proceedings of the 2020 ACM SIGSAC Conference on Computer and Communications Security*, pp. 1253–1269, 2020.
- [34] B. Choi, J.-y. Sohn, D.-J. Han, and J. Moon, “Communication-computation efficient secure aggregation for federated learning,” *arXiv preprint arXiv:2012.05433*, 2020.
- [35] X. Guo, Z. Liu, J. Li, J. Gao, B. Hou, C. Dong, and T. Baker, “V eri fl: Communication-efficient and fast verifiable aggregation for federated learning,” *IEEE Transactions on Information Forensics and Security*, vol. 16, pp. 1736–1751, 2020.
- [36] S. Kadhe, N. Rajaraman, O. O. Koyluoglu, and K. Ramchandran, “Fastsecagg: Scalable secure aggregation for privacy-preserving federated learning,” *arXiv preprint arXiv:2009.11248*, 2020.
- [37] J. C. Zhao, A. Sharma, A. R. Elkordy, Y. H. Ezzeldin, S. Avestimehr, and S. Bagchi, “Loki: Large-scale data reconstruction attack against federated learning through model manipulation,” in *2024 IEEE Symposium on Security and Privacy (SP)*, pp. 30–30, IEEE Computer Society, 2023.
- [38] S. Shi, N. Wang, Y. Xiao, C. Zhang, Y. Shi, Y. T. Hou, and W. Lou, “Scale-mia: A scalable model inversion attack against secure federated learning via latent space reconstruction,” *arXiv preprint arXiv:2311.05808*, 2023.
- [39] S. Anwar, A. Parida, S. Atito, M. Awais, G. Nino, J. Kitler, and M. Lingurar, “Spexr: Self-supervised pretraining using chest x-rays towards a domain specific foundation model,” 2023.